ChemComm

Structural Regulation of Zinc-Porphyrin Frameworks via the Auxiliary Nitrogen-containing Ligands towards the Selective Adsorption of Cationic Dyes

Journal:	*ChemComm*
Manuscript ID	CC-COM-03-2019-002405.R1
Article Type:	Communication

Journal Name

COMMUNICATION

Structural Regulation of Zinc-Porphyrin Frameworks via the Auxiliary Nitrogen-containing Ligands towards the Selective Adsorption of Cationic Dyes

Received 00th January 20xx,
Accepted 00th January 20xx

DOI: 10.1039/x0xx00000x

www.rsc.org/

Xiao-ning Wang,[a] Jiang-li Li,[a] Yu-meng Zhao,[a] Jian-dong Pang,[b] Bao Li[a,*], Tian-Le Zhang[a] and Hong-Cai Zhou[b,*]

Three Metal–Organic Frameworks have been synthesized by using the N-containing ligands and meso-tetra(4-carboxyphenyl)porphyrin , which all exhibit the distinct selective adsorption capacity toward various organic dyes, illustrating the most important influence of the structural characteristics.

In the past few decades, the emergence of Metal-Organic Frameworks (MOFs) crystalline materials with tunable pore size and modifiable pore surfaces has motivated the intensive interest owing to their widely potential applications.[1,2] In contrast to the extensive investigations focused on gas-adsorption properties[3], catalysis[4,5] as well as chemical sensing[6], studies over the application of MOFs in biomimicry and biological fields still remains relatively underdeveloped. The presented results have shown that the rational regulation of porous structure, chemical environment and surface functionality of pore channels of MOFs would facilitate their applications in biological field.[7]

Due to the intrinsic biological relevance, the incorporation of biomimic functionalities into MOF frameworks has been demonstrated as an efficient way to construct the nucleobase-incorporated MOFs.[7b] However, except for a limited number of flexible metal-peptide frameworks that mimic the conformational adaptability of proteins, nucleobase-incorporated MOFs has been rarely explored.[8] Recently, MOFs consisted of the substituted porphines and metalloporphyrins has received great attention due to their excellent structural-activity relationship.[9-11] Viewed from the presented structures, most of the porphyrinic MOFs exhibits the low-dimensional topologies and limited application due to their routine coordination habits. For example, the utilization of meso-tetra(4-carboxyphenyl)porphyrin (H_6TCPP) reacted with zinc ion tends to facilitate the two dimensional framework. To break through the bondage of the coordination pattern of these porphyrinic linkers, the introduction of versatile nitrogen-containing ligands that possess variable coordination modes would be of an effective way to further explore the structural diversities and functionalities of porphyrinic MOFs. Herein, in order to establish a successful demonstration about the synergistic effect between the porphyrine and auxiliary linkers, three microporous porphyrinic MOFs, $[(NH_2Me_2)][Zn_3(TCPP)(bentz)]$ (**1**), $[(NH_2Me_2)_2][Zn_{6.5}(TCPP)_{1.5}(tz)_6(H_2O)_6]$ (**2**) and $[(NH_2Me_2)_6][Zn_9(TCPP)_3(H_2O)_2(ade)_2(\mu_2\text{-}O)_2]$ (**3**), (bentz = benzotriazole, Htz = 1H-1,2,3-triazole, ade = adenine), had been synthesized (Scheme S1, ESI†). Structural characterizations reveal the specific synergistic effects caused by the combinations of TCPP and versatile zinc clusters. Especially for **3**, open Watson-Crick planar constructed by adenine and TCPP had been embellished periodically in the interior surface of the anionic framework, which might be responsible for the excellent adsorption of dye molecules.

Due to the distinct coordination habits of the selected auxiliary ligands, three new MOFs with the different zinc clusters and topological structures had been characterized. **1** crystallizes in the orthorhombic space group *Pnnm* with an asymmetric unit consisting of three Zn^{2+} ions, one TCPP and one benzotriazole (Figure S1a, ESI†). Zn1 and Zn3 atoms are five-coordinated with four oxygen atoms from different TCPP ligands and one nitrogen atom from benzotriazole. The typical $Zn_2(COO)_4$ paddle-wheel clusters had been fabricated via the symmetric growth of Zn1 or Zn3 atom, whose apical sites are occupied by benzotriazole molecules. Zn2 and Zn4 atoms are exclusively bind by four pyrrole nitrogen atoms. In this way, each TCPP connects four paddle-wheel clusters and chelates one zinc ion to form the 2D porphyrin layer. The benzotriazole ligands act as pillars, and extend the adjacent 2D layers to form

[a] Key laboratory of Material Chemistry for Energy Conversion and Storage, School of Chemistry and Chemical Engineering, Huazhong University of Science and Technology, Wuhan, Hubei, 430074, PR China. E-mail: libao@hust.edu.cn.

[b] Department of Chemistry, Texas A&M Energy Institute, Texas A&M University,College Station, Texas 77843-3255, United States. E-mail: zhou@chem.tamu.edu

† Footnotes relating to the title and/or authors should appear here.
Electronic Supplementary Information (ESI) available: Additional experimental sections, characterization and physical measurements (PDF). X-ray crystallographic data for **1-3** (CIF). CCDC 1848723-1848725. For ESI and crystallographic data in CIF or other electronic format see DOI: 10.1039/x0xx00000x

a 3D porous framework that contains 1D quadrangle microporous channels along the *c* axis (Fig. 1a). Zn-O and Zn-N distances fall in the range from 1.846(7) to 2.160(6) Å, while Zn···Zn distance is 2.9478(18) Å, in accordance with the typical values of Zn_2 cluster.[12] The total solvent accessible volume in **1** is ascertained to be 59% (11298.5 Å^3 /19070.5 Å^3), calculated by the *PLATON* routine.

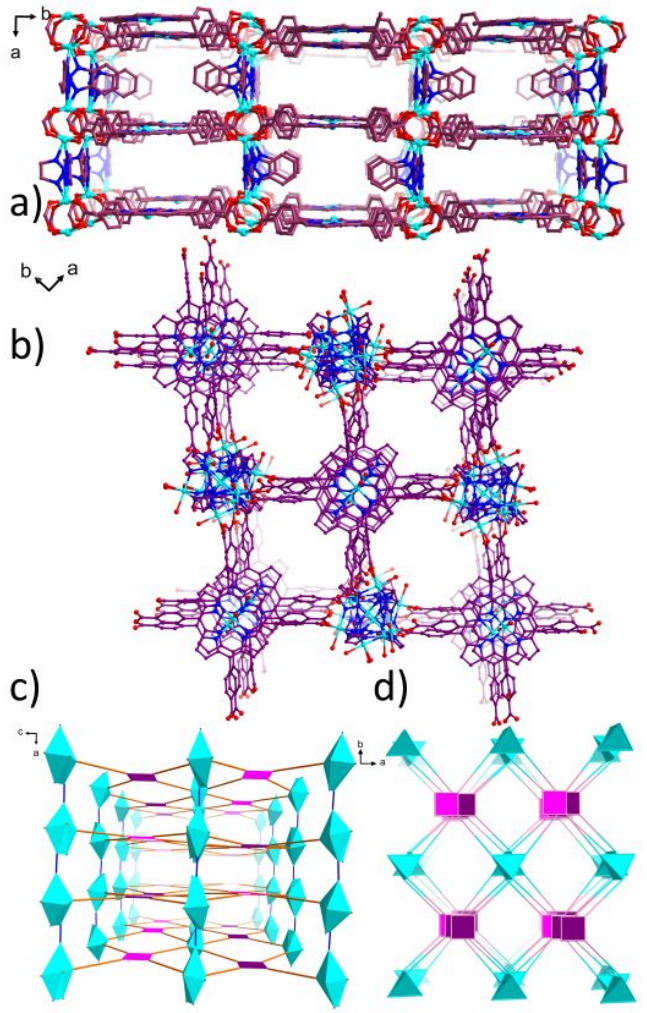

Fig. 1 (a) Partial view of the 3D framework of **1** along the *c* axis; (b) Partial view of the 3D framework of **2** along the *c* axis; (c) The topological network of **1**; (d) The topological network of **2**. (Purple square and green polyhedron represent TCPP and Zn cluster)

Comparably, **2** crystallizes in triclinic *P*-1 space group, which comprises six and half Zn^{2+} ions, one and half TCPP ligands, six tz ligands and six coordinated water molecules in one asymmetric unit (Figure S2a, ESI†). The vacancy of TCPP ligands have been occupied by zinc ions (Zn6 and Zn7). There are two types of the carboxylate groups on TCPP(Figure S3, ESI†): the carboxylate substitutes on one type of TCPP adapt the chelating mode to connect four Zn^{2+} ions; the other ones are the mono-dentate carboxylates to connect four Zn^{2+} ions. Furthermore, Zn1 and Zn4 atoms are five-coordinated with three nitrogen atoms from different tz, two oxygen atoms from one carboxylate and one coordinated water molecule. Zn2 and Zn3 atoms are six-coordinated with three nitrogen atoms from different tz, two carboxylate oxygen atom from two different TCPP ligands and one coordinated water molecule. Zn5 is exclusively coordinated by six nitrogen atoms from six tz, which locates in the center and connects other four zinc ions via tz to form the penta-nuclear $r[Zn_5(tz)_6]^{4+}$ clusters (Figure S2b, ESI†). The perpendicular of Zn5 cluster is further decorated by six TCPP ligands to generate a 3D framework, which possesses 1D rhombus-shaped channel along the *c* axis (Fig. 1b). A *PLATON* calculation indicates a solvent-accessible volume of approximately 65% (6286.1 Å^3 /9647.0 Å^3) in the final framework.

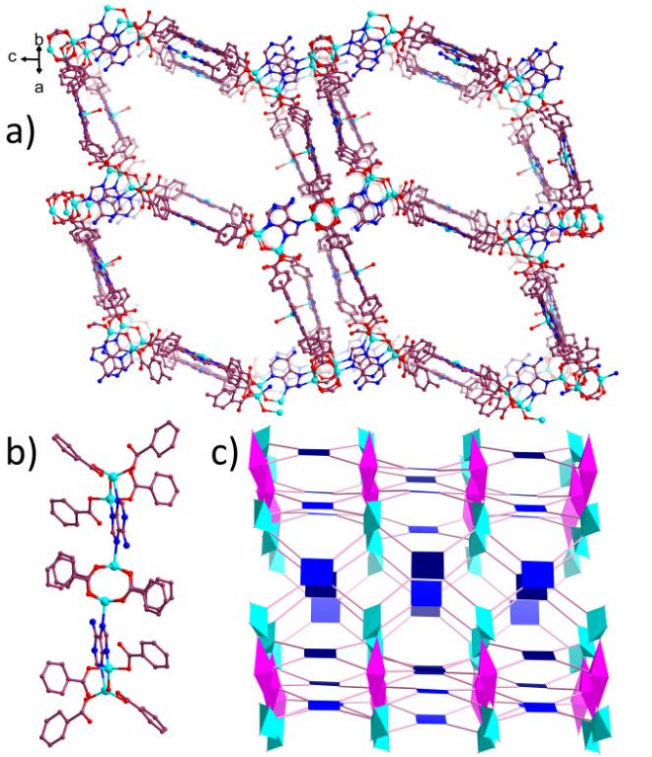

Fig. 2 (a) Partial view of the 3D framework of **3**; (b) A fragment showing the hexa-nuclear cluster, the open Watson-Crick faces and the uncoordinated carboxyl-O sites; (c) The topological network of **3**. (blue square represents TCPPP; purple and green polyhedrons represent Zn clusters)

Differently, **3** crystallizes in the triclinic *P*-1 space group (see Table S1, ESI†). The asymmetric unit of **3** contains nine Zn^{2+} ion, three TCPP ligands, two adenine ligands, two μ_2-O and two coordinated water molecules (Figure S4, ESI†). The vacancy of TCPP had been occupied by zinc ions (Zn7, Zn8 and Zn9).Three connection types of TCPP had been observed and illustrate in Figure S5, ESI†, which separately connects four, five and six zinc ions. Due to the synergistic effect between ade and TCPP, diverse connection modes and novel configurations of zinc clusters had been stabilized. The coordination sites of Zn1-Zn4 had been occupied by one adenine-N, two carboxylate O atoms from two TCPP ligands and one μ_2-O atom. Zn1 and Zn2/Zn3 and Zn4 are bind together to form the di-nuclear cluster via $\mu_{1,3}$-bridging ade and μ_2-O atom. Zn5 or Zn6 atoms adapts the tetragonal pyramid geometry to form the typical $Zn_2(COO)_4$ paddlewheel, whose axial positions are occupied by adenine-N

atoms. Through the connection of ade, the paddlewheel cluster had been extended to form the hexa-nuclear cluster (Fig. 2b), which is further decorated by twelve TCPP ligands to form the final framework. 1D rhombus-shaped channel had been left in the final framework (Fig. 2a). The open Watson-Crick faces and the uncoordinated carboxyl-O sites had been decorated on the surface of the channel, which endows **3** with the potential adsorption ability towards the specific molecules. A *PLATON* calculation indicates a solvent-accessible volume of approximately 75% (15858.2 Å^3 /21050.7 Å^3) in the final framework.

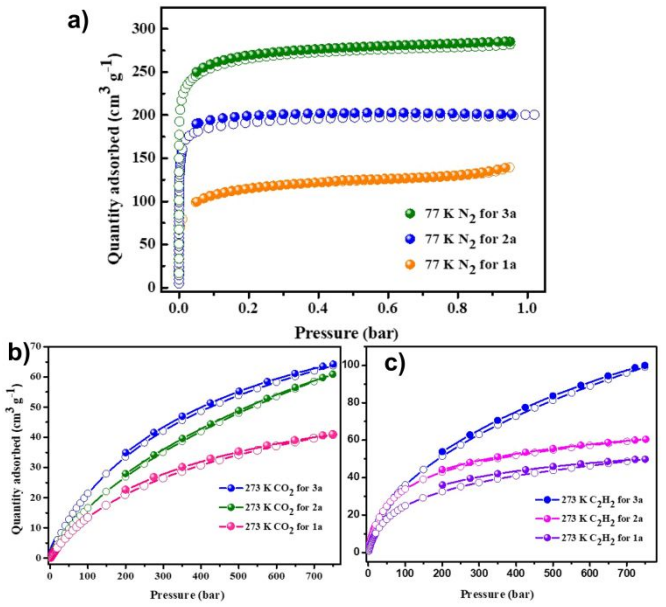

Fig. 3 N_2 physisorption isotherms for **1**-**3** at 77 K (a); CO_2 adsorption isotherms for **1**-**3** at 273 K (b); C_2H_2 adsorption isotherms for **1**-**3** at 273 K (c).

The purity of these synthesized samples had been checked via PXRD experiments (Figure S7-9, ESI†), which gives the matched spectra with the simulated ones. The thermal stability of these samples had been also measured (Figure S10-12, ESI†). Due to the introduction of auxiliary ligands, the high thermal stability had been presented for **1**-**3**. Thanks to the large channel and low framework density, the porous traits of these zinc-porphyrin frameworks had been characterized via N_2 adsorption at 77 K (Fig. 3a). The activated samples of **1-3** could adsorb 138, 200, 286 cm^3 g^{-1} N_2, respectively, along with the calculated BET surface area/Langmuir surface area of 373.5/551.4 m^2 g^{-1} for **1**, 456.1/678.2 m^2 g^{-1} for **2** and 622.8/918.5 m^2 g^{-1} for **3**. Furthermore, the type-I isotherms of N_2 adsorption illustrate the micro-porous characteristics for the activated **1**-**3**. Furthermore, these frameworks also exhibit the proper adsorption abilities towards the small molecules as CO_2 and C_2H_2, illustrating the existence of strong adsorption sites in the channels of frameworks. The increasing parameters of porous surfaces and amounts of the guest molecules are in consistent with the structural characteristics of three MOFs, further manifesting the important role of the auxiliary nitrogen-containing ligands to regulate the porous structures of Zinc-Porphyrin Frameworks.

The proper porous traits of these MOFs encouraged us to further explore the adsorption ability for dyes molecules with different size and charge. In order to acquire a systematic insight into the dye-adsorption properties for **1-3**, two comparable sets of tests had been carried out: In the first group, three dyes with the similar size and different charges (methylene blue: MB^+; neutral red: NR^0; methyl orange: MO^-) had been selected as the target guest molecules. The main absorption intensity of MB^+ at 664 nm significantly drops with the passage of time and the blue solution also faded to become colorless, indicating that MB^+ has been adsorbed by **1-3** via ion-exchange with $Me_2NH_2^+$ (Fig. 4a and Figure S16a,18a, ESI†). However, the unchanged concentration of NR^0 and MO^- indicate that the neutral NR and anionic MO^- dyes cannot be adsorbed by **1-3** although with the accessible sizes (Figure S13, 14, ESI†). These experimental results illustrate that the dye adsorption behaviors for 1-3 could only take place towards cationic ones, in consistent with the principle of ionic effect.

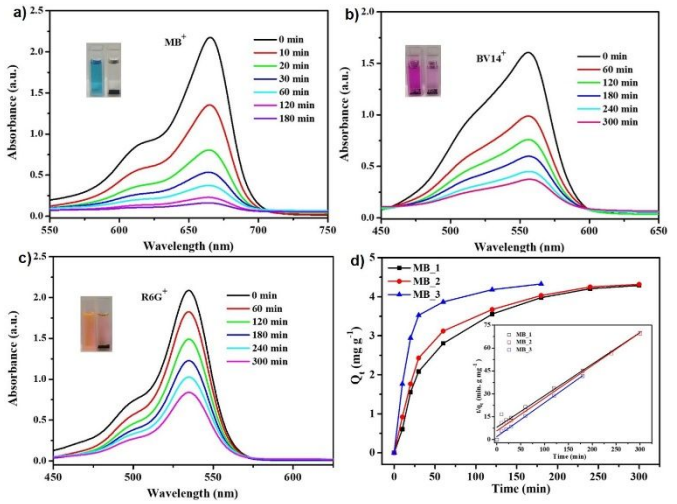

Fig. 4 UV-vis spectra of DMF solutions of methylene blue (MB^+) (a), basic violet 14 ($BV14^+$) (b), and rhodamine 6G ($Rh6G^+$) (c) in the presence of complex **3** at different times. The inset images display the change in colors before and after the dye adsorption by complex **3**. (d) Adsorption kinetics and the corresponding plots of pseudo-second order fitting plots of **1-3** towards MB.

To further verify the selectivity of dyes with different charges, the samples of **1-3** had been immersed in the mixtures of MB^+ and NR^0, MB^+ & MO^- with equal concentration, respectively (Fig. 5, Figure S17,19, ESI†). It is obviously that the adsorption intensity of the peak for MB^+ (664 nm) decreases along with the unchanged peaks for NR^0 (453 nm) and MO^- (421 nm). Meanwhile, the color of the mixed solutions slowly turned from green to orange after 5 h, respectively. This experimental phenomenon obviously illustrates the selective adsorption of different dye molecules, in consistent with the structural characteristics of **1**-**3** such as anionic framework and large porosity. Apart from this, the adsorption mechanism might be ascribed to the ion-exchange process, which endows **1-3** with the potential application as charge-dependent adsorbent for the selective separation of organic dyes.

The second set of dyes includes MB^+, basic violet 14 ($BV14^+$) and rhodamine 6G ($R6G^+$), which have the same charge but

different sizes (Table S5, ESI†). The adsorption experiments manifested that all of these MOFs exhibit the quick adsorption ability (Fig. 4, Figure S16, 18, ESI†), but with the different adsorption degree for three cationic dyes. For MB^+, 91.1%, 91.3% and 92% of dye concentration can be absorbed by the solid samples of **1-3** after 5 h, respectively, illustrating the excellent adsorption abilities of these MOFs. For $BV14^+$ and $R6G^+$ under the same testing conditions, the adsorption ratio of **1-3** were calculated to be 64%, 70.8%, and 75.8% as well as 35.8%, 50%, and 59.5%, respectively. The kinetic rate constants for the adsorption of three dyes in 1-3 had been calculated, in consistent with the marcoscopic phenomenons (Table S6, ESI†). The difference should be ascribed to the sized effect of dyes (Table S5, ESI†). The smallest MB^+ molecules are able to easily enter into the pore of these MOFs, which gives the largest kinetic rate constant compared to other two dyes. In addition, the largest pore dimension in **3** must be responsible for the better adsorption efficiency towards the larger dyes as $BV14^+$ and $R6G^+$ compared to **1** and **2**.

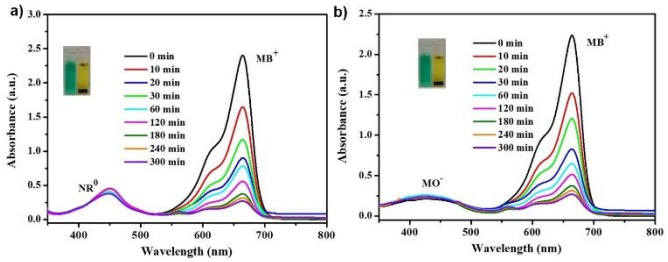

Fig. 5 UV-Vis absorption spectra of equimolar MB^+ & NR^0 (a) and MB^+ & MO^- (b) in the presence of the complex **3** at different times. The inset images display the change in colors before and after the dye adsorption by complex **3**.

In summary, by introducing the versatile auxiliary ligands, three novel zinc-porphyrin MOFs had been constructed. All of these MOFs exhibit the distinct 3D extended structures fabricated including the different zinc clusters and topological structures, which must be ascribed to the synergistic effect between the porphyrinic linker and versatile N-donor ligands. Especially for **3**, the open Watson-Crick planar in the interior surface has been presented. Benefiting from the structural traits as the high porosity and anionic framework, all of these MOFs can selectively adsorb cationic organic dyes in solution. The pore dimension and charged framework must be responsible for the origination of the different adsorption behaviors. The presented results have expanded the coordination diversities of porphyrin-based MOFs, and illustrating the important role of the synthesis strategy for fabricating the anticipated MOF materials.

We gratefully acknowledge the National Natural Science Foundation of China (No. 21471062), the Center for Gas Separations Relevant to Clean Energy Technologies, an Energy Frontier Research Center (EFRC) funded by the U.S. Department of Energy (DOE), Office of Science, and Office of Basic Energy Sciences (DESC0001015), Office of Fossil Energy, the National Energy Technology Laboratory (DE-FE0026472), and the Robert A. Welch Foundation through a Welch Endowed Chair to HJZ (A-0030) for financial support, and the Analytical and Testing Center, Huazhong University of Science and Technology, for analysis and spectral measurements.

Conflicts of interest

There are no conflicts to declare.

Notes and references

1 (a) S. Kitagawa and K. Uemura, *Chem. Soc. Rev.*, 2005, **34**, 109; (b) G. Férey and C. Serre, *Chem. Soc. Rev.*, 2009, **38**, 1380; (c) H. C. Zhou, J. R. Long and O. M. Yaghi, *Chem. Rev.*, 2012, **112**, 673.

2 (a) K. Sumida, D. L. Rogow, J. A. Mason, T. M. McDonald, E. D. Bloch, Z. R. Herm, T.-H. Bae and J. R. Long, *Chem. Rev.*, 2012, **112**, 724; (b) J.-R. Li, J. Sculley and H.-C. Zhou, *Chem. Rev.*, 2012, **112**, 869.

3 (a) L. Zhang, K. Jiang, L. Li, Y. Xia, T. Hu, Y. Yang, Y. Cui, B. Li, B. Chen and G. Qian, *Chem. Commun.*, 2018, **54**, 4846; (b) K. Adil, Y. Belmabkhout, R. S. Pillai, A. Cadiau, P. M. Bhatt, A. H. Assen, G. Maurin and M. Eddaoudi, *Chem. Soc. Rev.*, 2017, **46**, 3402.

4 (a) Y. Yang, C. Gao, H. Tian, J. Ai, X. Min and Z. Sun, *Chem. Commun.*, 2018, **54**, 1758; (b) J. Liu, L. Chen, H. Cui, J. Zhang, L. Zhang and C. Y. Su, *Chem. Soc. Rev.*, 2014, **43**, 6011; (c) J. Baek, B. Rungtaweevoranit, X. Pei, M. Park, S. C. Fakra, Y. Liu, R. Matheu, S. A. Alshmimri, S. Alshehri, C. A. Trickett, G. A. Somorjai and O. M. Yaghi, *J. Am. Chem. Soc.*, 2018, **140**, 18208.

5 (a) M. J. Katz, S. Moon, J. E. Mondloch, M. H. Beyzavi, C. J. Stephenson, J. T. Hupp and O. K. Farha, *Chem. Sci.*, 2015, **6**, 2286. (b) M. Ding and H. Jiang, *ACS. Catal.*, 2018, **8**, 3194. (c) Q. Yang, Q. Xu and H. Jiang, *Chem. Soc. Rev.*, 2017, **46**, 4774. (d) Y. Huang, J. Liang, X. Wang and R. Cao, *Chem. Soc. Rev.*, 2017, **46**, 126.

6 (a) Y. Cui, Y. Yue, G. Qian and B. Chen, *Chem. Rev.*, 2011, **112**, 1126; (b) Z. Hu, B. J. Deibert and J. Li, *Chem. Soc. Rev.*, 2014, **43**, 5815; (c) W. P. Lustig, S. Mukherjee, N. D. Rudd, A. V. Desai, J. Li and S. K. Ghosh, *Chem. Soc. Rev.*, 2017, **46**, 3242.

7 (a) M. Zhang, Z. Gu, M. Bosch, Z. Perry and H. Zhou, *Coord. Chem. Rev.*, 2015, **293**, 327; (b) I. Imaz, M. Rubio-Martínez, J. An, I. Solé-Font, N. L. Rosi and D. Maspoch, *Chem. Commun.*, 2011, **47**, 7287.

8 (a) G. Beobide, O. Castillo, J. Cepeda, A. Luque, S. Pérez-Yáñez, P. Román, J. Thomas-Gipson, *Coord. Chem. Rev.*, 2013, **257**, 2716; (b) P. Amo-Ochoa and F. Zamora, *Coord. Chem. Rev.*, 2014, **276**, 34.

9 (a) M. H. Beyzavi, N. A. Vermeulen, A. J. Howarth, S. Tussupbayev, A. B. League, N. M. Schweitzer, J. R. Gallagher, A. E. Platero-Prats, N. Hafezi, A. A. Sarjeant, J. T. Miller, K. W. Chapman, J. F. Stoddart, C. J. Cramer, J. T. Hupp and O. K. Farha, *J. Am. Chem. Soc.*, 2015, **137**, 13624. (b) J. A. Johnson, B. M. Petersen, A. Kormos, E. Echeverría, Y. Chen and J. Zhang, *J. Am. Chem. Soc.*, 2016, **138**, 10293. (c) G. Lin, H. Ding, D. Yuan, B. Wang and C. Wang, *J. Am. Chem. Soc.*, 2016, **138**, 3302; (d) S. Huh, S. -J. Kim and Y. Kim, *CrystEngComm*, 2016, **18**, 345.

10 (a) J. Pang, S. Yuan, J. Qin, M. Wu, C. T. Lollar, J. Li, N. Huang, B. Li, P. Zhang and H. Zhou, *J. Am. Chem. Soc.*, 2018, **140**, 12328; (b) P. Deria, D. A. Gómez-Gualdrón, I. Hod, R. Q. Snurr, J. T. Hupp and O. K. Farha, *J. Am. Chem. Soc.*, 2016, **138**, 14449; (c) W. Morris, B. Volosskiy, S. Demir, F. Gándara, P. L. McGrier, H. Furukawa, D. Cascio, J. F. Stoddart and O. M. Yaghi, *Inorg. Chem.*, 2012, **51**, 6443.

11 (a) N. Huang, K. Wang, H. Drake, P. Cai, J. Pang, J. Li, S. Che, L. Huang, Q. Wang and H. Zhou, *J. Am. Chem. Soc.*, 2018, **140**, 6383; (b) Z. Zhang, L. Zhang, L. Wojtas, P. Nugent, M. Eddaoudi and M. J. Zaworotko, *J. Am. Chem. Soc.*, 2011, **134**, 924.

12 (a) G. Dutta, A. K. Jana and S. Natarajan, *Chem. - Eur. J.,* 2017, **23**, 8932; (b) W. Fan, H. Lin, X. Yuan, F. Dai, Z. Xiao, L. Zhang, L. Luo and R. Wang, *Inorg. Chem.*, 2016, **55**, 6420.

Structural Regulation of Zinc-Porphyrin Frameworks via the Auxiliary Nitrogen-containing Ligands towards the Selective Adsorption of Cationic Dyes

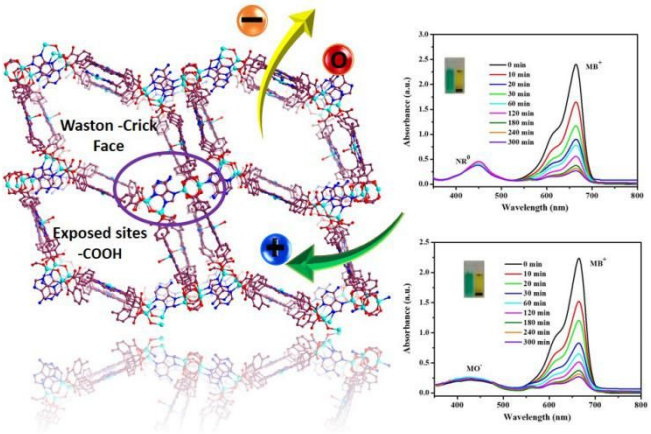

Three novel zinc-porphyrin MOFs have been synthesized by using versatile N-containing ligands. The open Watson-Crick planar in the interior surface in one Zn-MOF has been presented, which could endow the related MOF with the excellent selective adsorption of dye molecules.